IDENTIFICATION OF MULTILOOP PILOT DESCRIBING FUNCTIONS

OBTAINED FROM SIMULATED APPROACHES TO AN AIRCRAFT CARRIER

Wayne F. Jewell

Systems Technology, Inc.

SUMMARY

This paper presents some predicted results of a simulation of the carrier aircraft pilot's approach control strategy in the presence of pilot remnant. The aircraft dynamics and the turbulence environment are representative of a trainer-type aircraft. The Non-Intrusive Pilot Identification Program (NIPIP) was used to identify the pilot's control strategy required by this highly-coupled, multiloop control task. The results are presented in terms of frequency responses of the individual elements of the pilot's control strategy and indicate that NIPIP can identify the pilot's describing functions even in the presence of significant amounts of pilot remnant. The next step is to apply NIPIP to a real time, piloted simulation of the same control task. This is planned for the Visual Technology Research Simulator at the Naval Training Equipment Center in Orlando, Florida.

INTRODUCTION

The Non-Intrusive Pilot Identification Program (NIPIP) was developed, evaluated, and applied to a simulated approach and landing of a conventional takeoff and landing (CTOL) aircraft (Refs. 1 and 2). The performance evaluation of NIPIP demonstrated that accurate, unbiased estimates of the pilot's input-output describing function, Y_p, could be obtained without explicit knowledge of the disturbance function (Refs. 1 and 2). The atmospheric disturbance was injected into the aircraft dynamics (instead of being injected into the control loop) and was not used as an input to NIPIP. NIPIP obtained the pilot's input-output describing function by using a time-domain model of Y_p and a least-squares identification algorithm. Furthermore NIPIP used a "sliding" time window to estimate Y_p enabling it to identify time-varying behavior in the pilot's control strategy.

Although the CTOL control task of Refs. 1 and 2 was a multiloop manual control problem, there was very little coupling between the fast/slow (throttle) axis and the flight director (column) axis. In effect, two single axis manual control tasks were being performed simultaneously. In the present case of carrier landing, however, the block diagram in Fig. 1 depicts the highly-coupled, multiloop manual control task used by Navy pilots for final approach. The prescribed Navy piloting technique for controlling the aircraft is to regulate glide slope deviation, d, with throttle, δ_T, and angle of attack, α, with commanded pitch attitude, θ_c. Commanded pitch attitude, in turn, is regulated with the elevator, δ_E, as shown in Fig. 1 (Ref. 3). In reality, however, a pilot learns that he must "crossfeed" the controls in order to "stay ahead" of the aircraft; that is, when the pilot makes a correction to d using δ_T he also adjusts θ_c, as shown in Fig. 1.
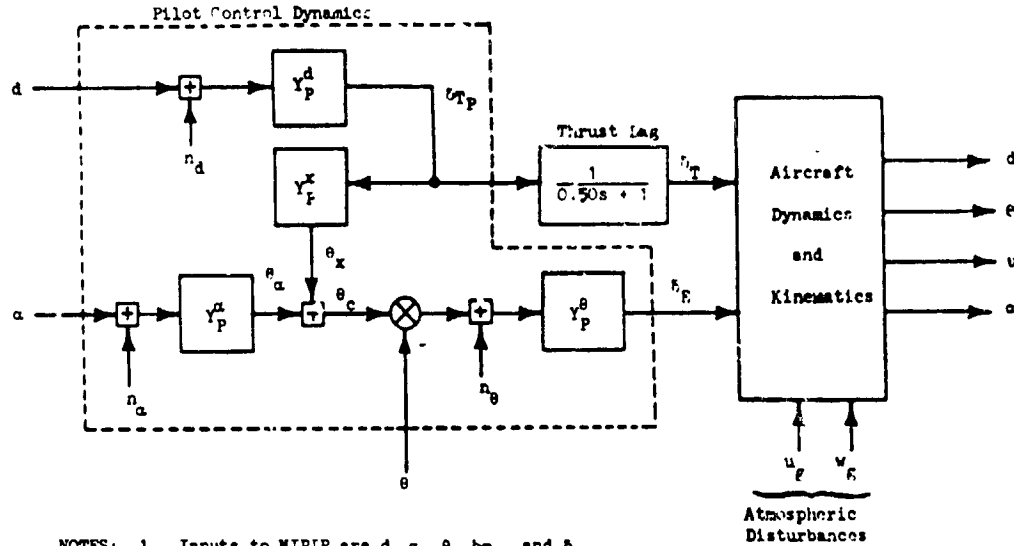
NOTES: 1. Inputs to NIPIP are d, α, θ, b_{T_P}, and δ_E

2. Output from NIPIP are $\hat{Y}_P^\alpha$, $\hat{Y}_P^\theta$, $\hat{Y}_P^d$, and $\hat{Y}_P^X$

Figure 1. Manual Control Task for STOL Approach and Landing

The analytical study by Heffley, et al., in Ref. 4 demonstrates that
the "pursuit-crossfeed" piloting technique described above, and shown in
Fig. 1, must be used in order to obtain adequate approach precision. How-
ever significant skill development is required to adopt the proper crossfeed
for the aircraft and approach speed being flown. If the pilot is required
to fly a different aircraft, as is done when proceeding from a trainer to a
fleet aircraft, he must readapt his crossfeed gain. Furthermore Ref. 4
shows that compensatory Y_P^α can become a very low and almost negligible gain
when the pilot has learned to develop the pursuit crossfeed, Y_P^X.

To prepare for identifying skill development in the pilot's control
strategy, NIPIP was used first in an inanimate simulation in scaled time to
quantify the various elements of the pilot's control technique; i.e., Y_P^d,
Y_P^X, Y_P^α, and Y_P^θ in Fig. 1 in the presence of pilot remnant. Our ultimate
goal is to use NIPIP for analyzing simulated approaches to an aircraft car-
rier in real time using the Visual Technology Research Simulator (VTRS,
Ref. 5) at the Naval Training Equipment Center (NTEC) in Orlando, Florida.
This will be done within the near future using Navy pilots and a number of
simulated aircraft.

Prior to using NIPIP in conjunction with the piloted simulation de-
scribed above, we wanted to know if NIPIP could indeed identify the indi-
vidual elements of the complex control loop structure shown in Fig. 1. In
order to prove NIPIP's ability to do this, we simulated the aircraft dynam-
ics, the pilot describing functions, and the pilot remnant shown in
Fig. 1. The combined pilot-aircraft system was disturbed with simulated
atmospheric turbulence. The results of analyzing this data are presented in
the remainder of this paper.

TECHNICAL APPROACH

The aircraft dynamics used in the simulation were representative of a T2-C at 108 kt, flaps fully extended (Ref. 6). The various pilot describing functions indicated in Fig. 1 were as follows:

$$Y_P^\theta = -0.30 \frac{s + 10.0}{s + 3.0} \left(\text{rad } \delta_E / \text{rad } \theta_e \right)$$

$$Y_P^d = 32.6 \frac{2.0}{s + 2.0} \left(\text{lb } \delta_T / \text{ft d} \right)$$

$$Y_P^{\ddot{x}} = 8.2\text{E-5} \frac{3.0}{s + 3.0} \left(\text{rad } \theta_x / \text{lb } \delta_{T_P} \right)$$

$$Y_P^\alpha = 0.0$$

The compensation defined above yields a pitch-loop bandwidth of about 3.0 rad/sec and a glide slope loop bandwidth of about 0.50 rad/sec. The angle of attack loop was not closed for the results presented herein (it is a very low bandwidth loop) but will be added in the future. The crossfeed was designed such that the steady-state airspeed will remain unchanged for any amount of throttle deflection. It should be mentioned that, from a control system design point of view, it is possible to use pure gains for Y_P^θ, Y_P^d, and Y_P^x. However this would have been a trivial identification problem for NIPIP and would not necessarily be representative of human pilot dynamics.

Pilot remnant was simulated using shaped white noise and injected into the control loops as shown in Fig. 1. The shaping filters used to obtain n_θ and n_d were (Ref. 7)

$$\frac{n_d}{n_d} = \frac{2.58}{s + 3.33} \sigma_{n_d}$$

$$\frac{n_\theta}{n_\theta} = \frac{1.41}{s + 1.0} \sigma_{n_\theta}$$

where n_d and n_θ are independent white noise sources and σ_{n_d} and σ_{n_θ} are the rms values of n_d and n_θ. The values of σ_{n_d} and σ_{n_θ} were set such that

$$\sigma_{n_d} \doteq 0.25 \ \sigma_d$$

$$\sigma_{n_\theta} \doteq 0.25 \ \sigma_\theta$$

where σ_d and σ_θ are the rms values of d and θ when no remnant is present.

The atmospheric turbulence was simulated using pseudo-random noise (sum of sine waves) to simulate the axial, u_g, and the vertical, w_g, gusts. The

rms values for both u_g and w_g were 3.0 fps for the results contained here-in. The bandwidths of both u_g and w_g were about 0.50 rad/sec.

RESULTS

Some typical time histories of the pilot-aircraft response to turbulence with and without simulated pilot remnant are shown in Fig. 2. Note that the remnant has a fairly large effect on the controls, δ_T and δ_E, but a relatively small effect on the aircraft response. This is because the aircraft acts as a filter and smooths the noisy control inputs. The δ_T response looks granular because a sampling rate of 0.50 sec was deliberately used to simulate Y_p^d. A sampling rate of 0.10 sec was used to simulate Y_p^θ.
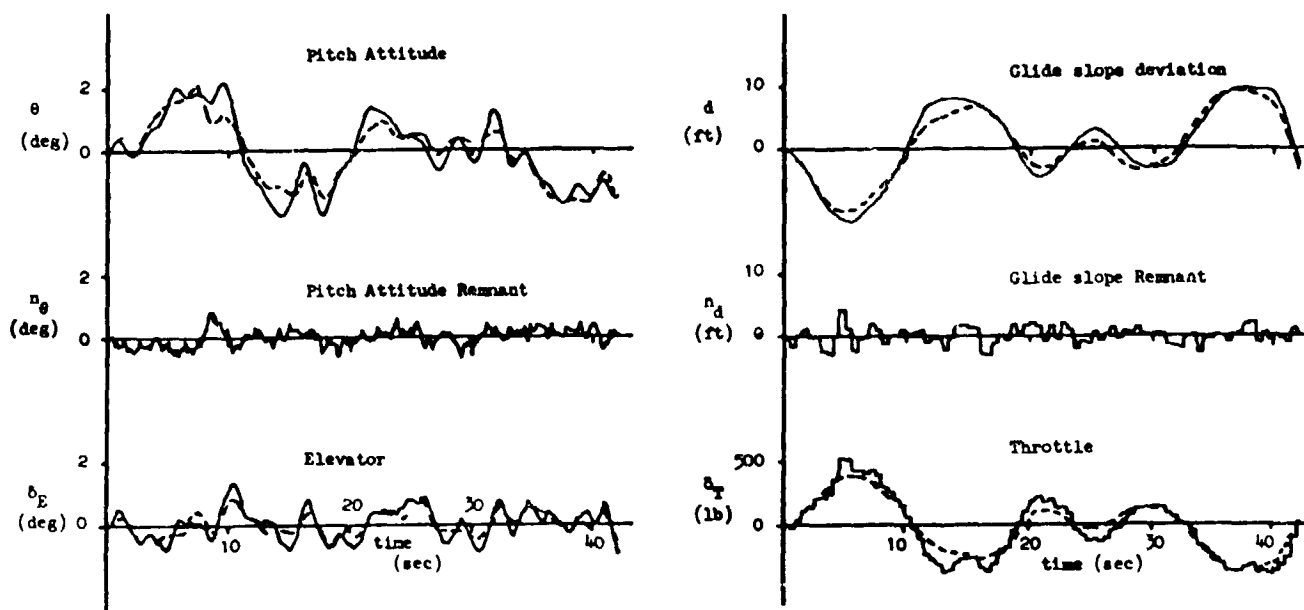
Figure 2. Pilot-Aircraft Response to Turbulence with and Without
Simulated Pilot Remnant

The time histories of d, δ_T, θ, and δ_E shown in Fig. 2 were used as inputs to NIPIP, from which NIPIP computed the desired pilot describing functions, Y_p^θ, Y_p^x, and Y_p^d. A detailed discussion of how NIPIP performs these calculations can be found in Ref. 2 and will not be repeated here.

Figures 3, 4, and 5 compare the frequency responses of the actual pilot dynamics to the outputs of NIPIP. The length of the time windows used in computing Y_p^θ and Y_p^x was 30 sec, but was 60 sec for Y_p^d. The longer time window was used for computing Y_p^d because the d → δ_T loop has a much lower bandwidth than the θ → δ_E loop. The three estimates of $Y_p(j\omega)$ shown in the figures demonstrate how the NIPIP outputs vary with time (even though the simulated pilot describing functions were stationary). The variation of all three estimates is fairly low, especially in the neighborhood of the cross-over frequency. The explanation for these phenomena is the more adverse signal-to-noise ratios outside the region of the crossover frequency. This result was also demonstrated in Ref. 2.
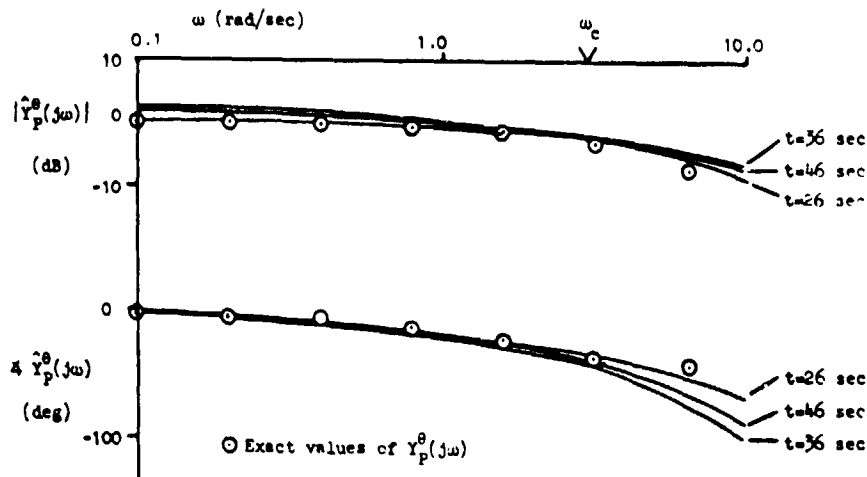
Figure 3. Frequency Response of $\hat{Y}_\theta$ with 25 Percent Remnant and a Time Window of 30 sec
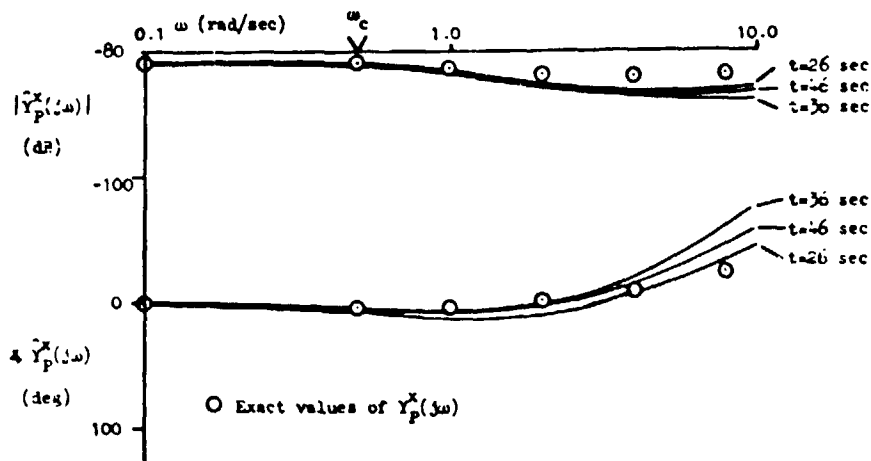
Figure 4. Frequency Response of $\hat{Y}_P^x$ with 25 Pe   nt Remnant and a Time Window of 30 sec

CONCLUDING REMARKS

The Non-Intrusive Pilot Identification Program (NIPIP) was used to estimate the pilot's control strategy required for the final approach and landing on an aircraft carrier. The estimates for the pilot's describing functions are quite accurate in the region of their respective crossover frequencies, $\left(\text{i.e., } \omega_d \text{ and } \omega_\theta\right)$. The errors could be further reduced by increasing the lengths of the time window. The penalty for doing this, however, is that any time-variation in the pilot's actual control strategy tends to be masked. The issue of time-variation in piloting technique will be addressed when we analyze the data from a piloted simulation on the Visual Technology Research Simulator at the Naval Training Equipment Center in Orlando, Florida.
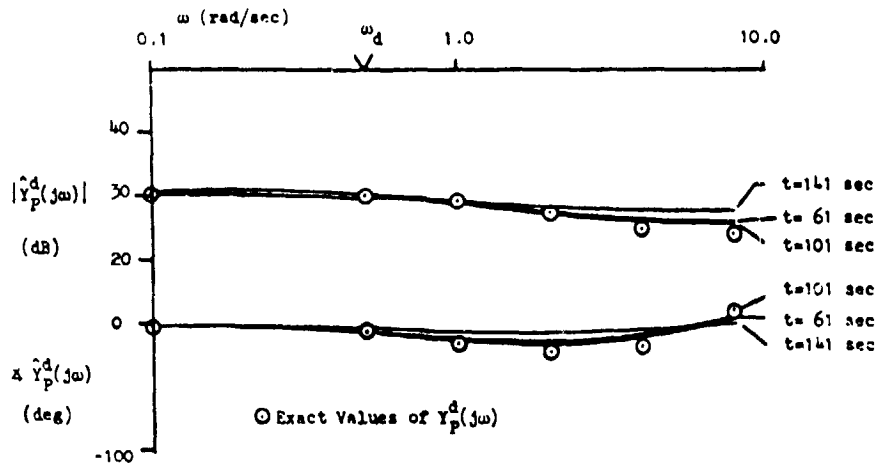
Figure 5. Frequency Response of $\hat{Y}_P^d(j\omega)$ with 25 Percent Remnant

REFERENCES

1. Jewell, Wayne F., "Application of a Pilot Control Strategy Identification Technique to a Joint FAA/NASA Ground-Based Simulation of Head-Up Displays for CTOL Aircraft," Sixteenth Annual Conference on Manual Control, MIT, Cambridge, Mass., May 5-7, 1980, pp. 395-409.

2. Jewell, Wayne F., and Schulman, Ted M., A Pilot Control Strategy Identification Technique for Use in Multiloop Control Tasks, Systems Technology, Inc., Technical Report No. 1153-2 (forthcoming NASA Contractor Report), May 1980.

3. Anon., Undergraduate Pilot Training Task Analysis, Phase II Report, Hq. Chief of Naval Air Training, NAS, Corpus Christi, Texas, July 1975.

4. Heffley, Robert K., Clement, Warren F., and Craig, Samuel J., "Training Aircraft Design Considerations Based on the Successive Organization of Perception in Manual Control," Sixteenth Annual Conference on Manual Control, MIT, Cambridge, Mass., May 5-7, 1980, pp. 119-127.

5. Chambers, Walt S., "AWAVS: An Engineering Simulator for Design of Visual Flight Training Simulators," J. of Aircraft, Vol. 14, No. 11, November 1977, pp. 1060-1063.

6. Buenz, D. A., et al., Identification of T-2 Aerodynamic Derivatives from Flight Data, Systems Control Inc., for Naval Air Development Center, March 1975 (AD-A021 996).

7. McRuer, D. T., and Krendel, E. S., Mathematical Models of Human Pilot Behavior, AGARD-AG-188, January 1974.